

Article

Comprehensive Genomic Analysis of Trihelix Family in Tea Plant (*Camellia sinensis*) and Their Putative Roles in Osmotic Stress

Zhuoliang Lang ^{1,2,†}, Zelong Xu ^{2,3,†}, Linying Li ², Yuqing He ² , Yao Zhao ² , Chi Zhang ² , Gaojie Hong ^{1,2,*}  and Xueying Zhang ^{2,*}

¹ College of Tea Science and Tea Culture, Zhejiang A&F University, Hangzhou 311300, China

² State Key Laboratory for Managing Biotic and Chemical Threats to the Quality and Safety of Agro-Products, Institute of Virology and Biotechnology, Zhejiang Academy of Agricultural Sciences, College of Advanced Agricultural Sciences, Zhejiang A&F University, Hangzhou 311300, China; anran6297@163.com (L.L.)

³ College of Advanced Agricultural Sciences, Zhejiang A&F University, Hangzhou 311300, China

* Correspondence: gjhong@126.com (G.H.); zhangxueying89@163.com (X.Z.); Tel.: +86-571-86419210 (X.Z.)

† These authors contributed equally to this work.

Abstract: In plants, Trihelix transcription factors are responsible for regulating growth, development, and reaction to various abiotic stresses. However, their functions in tea plants are not yet fully understood. This study identified a total of 40 complete Trihelix genes in the tea plant genome, which are classified into five clades: GT-1 (5 genes), GT-2 (8 genes), GT γ (2 genes), SH4 (7 genes), and SIP1 (18 genes). The same subfamily exhibits similar gene structures and functional domains. Chromosomal mapping analysis revealed that chromosome 2 has the most significant number of trihelix family members. Promoter analysis identified cis-acting elements in *C. sinensis* trihelix (CsTH), indicating their potential to respond to various phytohormones and stresses. The expression analysis of eight representative CsTH genes from four subfamilies showed that all CsTHs were expressed in more tissues, and three CsTHs were significantly induced under ABA, NaCl, and drought stress. This suggests that CsTHs plays an essential role in tea plant growth, development, and response to osmotic stress. Furthermore, yeast strains have preliminarily proven that CsTH28, CsTH36, and CsTH39 can confer salt and drought tolerance. Our study provides insights into the phylogenetic relationships and functions of the trihelix transcription factors in tea plants. It also presents new candidate genes for stress-tolerance breeding.

Keywords: *C. sinensis*; expression profile; phylogenetic analysis; trihelix family (TH); osmotic stress



Citation: Lang, Z.; Xu, Z.; Li, L.; He, Y.; Zhao, Y.; Zhang, C.; Hong, G.; Zhang, X. Comprehensive Genomic Analysis of Trihelix Family in Tea Plant (*Camellia sinensis*) and Their Putative Roles in Osmotic Stress. *Plants* **2024**, *13*, 70. <https://doi.org/10.3390/plants13010070>

Academic Editor: Vladimir V. Kuznetsov

Received: 1 November 2023

Revised: 21 December 2023

Accepted: 21 December 2023

Published: 25 December 2023



Copyright: © 2023 by the authors. Licensee MDPI, Basel, Switzerland. This article is an open access article distributed under the terms and conditions of the Creative Commons Attribution (CC BY) license (<https://creativecommons.org/licenses/by/4.0/>).

1. Introduction

Trihelix transcription factors, a plant-specific family of transcription factors, are characterized by their conserved three-helical structure (helix-loop-helix-loop-helix) [1]. These factors are commonly referred to as a GT factor family because they can bind to light-responsive elements (GT elements) [2]. The amino acid sequences of the N-terminal are generally consistent and strongly conserved, but the C-terminal are varied [3]. These transcription factors are generally classified into five subfamilies: GT1, GT2, GT γ , SH4, and SIP1 [1,4]. In contrast to the GT2 subfamilies, which possess two DNA-binding domains (one α -helix domain positioned at the center and the other in the C-terminus), the remaining subfamilies exclusively harbor a single (α -helix domain) in the C-terminal [3].

The first trihelix transcription factor, discovered in peas, was named GT1 [2]. The subsequent characterization of the tobacco GT1 revealed an α -helix domain in the C-terminus [5]. In contrast to GT1, GT2, a trihelix transcription factor in rice, exhibits distinct sequence preferences [6]. The GT1 and SH4 subfamilies' trihelix domains harbor a tryptophan residue within the interior hydrophobic region of the tandem repeat [7]. Although

the SH4 family possesses a more extended domain as compared to the others, the proteins of other subfamilies share an additional α -helix structure downstream of the conserved functional structural domain [8]. The third conserved tryptophan in the GT γ and GT2 subfamilies is replaced by phenylalanine, while it is substituted by isoleucine in the SIP1 subfamily [3,9].

The trihelix family is a small gene family with a relatively modest number of members, ranging from 30 to 60 members in most plant species as compared to other gene families. For instance, *Arabidopsis* possesses 29 members, rice harbors 41 members, poplar possesses 56 members, sorghum contains 40 members, maize has 44 members, chrysanthemum has 20 members, *Oenothera fragrans* has 56 members, and quinoa has 47 members [10–17]. Previous research has demonstrated the crucial role of trihelix transcription factors in plant development. ASIL2 (*Arabidopsis* 6b interacting protein-like2) regulates early embryo development, while ASIL1 exerts negative regulatory control over seedling embryo shape and maintains seed germination under temporal control [18]. *Arabidopsis* PTL (PETAL LOSS) deletion results in fewer petals. NtSIP1 (seed imbibition protein 1) is involved in plant cell proliferation [19]. Tomato SlGT11 plays a role in floral organ identity and the maintenance of floral characteristics [20,21].

Researchers have recently gained a heightened interest in the trihelix family genes due to their critical involvement in abiotic stressors. AtGT4, GhGT26, OsGT γ -1, and OsGT γ -2 enhance plant salt-stress tolerance [22–25]. The *Arabidopsis* SIP1 subfamily member gene, AtAST1, enhances salt and osmotic tolerances in transgenic plants by regulating stress-responsive genes [26]. AtGTL1 negatively regulates water use efficiency and drought tolerance in *Arabidopsis* by modulating stomatal density [27]. BnSIP1-1 (*Brassica napus*) is induced by ABA (Absciscic acid) and abiotic stress, and it improves seed germination when exposed to osmotic pressure, salt, and ABA treatments [28]. TaGT2L1 negatively regulates drought tolerance and stomatal development in wheat [29]. The overexpression of GmGT-2A, GmGT-2B, Sb06g023980, and Sb06g024110 can enhance *Arabidopsis*'s tolerance to salt, low temperature, and drought stress [4,30]. ZmGT-3b knockdown seedlings exhibit improved drought tolerance [31]. Ptagt1l regulates stomatal development and plant water absorption in *Populus trichocarpa* [32].

The increasing frequency and severity of high temperatures and drought stress impacts plants' growth, development, yield, and quality [33–35]. Most trihelix genes in *Brassica napus* exhibited significant changes in expression patterns upon heat treatment [36]. Additionally, the expression of 12 SbTHs was significantly upregulated in sorghum in response to high-temperature stress [13]. GT-1 acts as a mediator that links the signal perception and activation of the cellular thermal response by activating the expression of HsfA2 (Heat shock factor A2), a crucial factor for thermotolerance [37]. Persian walnut, a woody economic crop, enhances its tolerance to osmotic stress by regulating stomatal characteristics, maintaining ionic homeostasis, activating stress-responsive genes, and accumulating secondary metabolites [38,39]. The tea plant is a globally consumed cash crop renowned for its abundance of secondary metabolites, which contribute to its nutrient content, refreshing taste, and rich flavors that are beneficial to human health [40]. As a woody crop grown and cultivated in both tropical and temperate regions, tea plants have evolved a sophisticated suite of defense mechanisms to mitigate the effects of changing environmental stresses, such as extreme high temperatures and drought [41,42]. However, tea cultivation has expanded into areas with less-than-ideal conditions, leading to excessive salt stress in some regions. Salt stress is an environmental factor that disrupts ion transport and compromises tea plant photosynthesis.

The recently completed genome sequencing of *C. sinensis* has paved the way for unprecedented genome-wide characterization and the analysis of the repertoire of transcription factor families, including those crucial for modulating responses to diverse abiotic stressors. Given the potential roles of the trihelix family genes in stress tolerance, genome-wide analysis of CsTH genes is essential for further research. In this study, we identified a total of 40 potential trihelix genes. We comprehensively analyzed the sequence characteris-

tics, phylogenetic relationships, gene structure, chromosome distribution, and conserved motifs of the CsTH. Additionally, the expression profile of CsTH genes was examined in both the genes' normal and stressed states in response to salt and drought stress. These findings provide crucial data for further research into the functional genes of CsTH and offer potential gene resources for developing tea plant strains with enhanced stress tolerance.

2. Results

2.1. Identification and Classification of CsTH Genes in Tea Plants

A total of 40 non-redundant trihelix genes were identified from the genomic and transcriptome database of the tea plant, and their corresponding amino acid sequences matched the ASIL1/2-like (IPR044823) domain and possessed the MYB_DNA-binding domain (IPR044822). All the 40 CsTH genes contained the MYB_DNA-binding domain, and 16 of the genes had the ASIL1/2-like domain. We named these identified TH genes (CsTH1 to CsTH40) according to their location in the chromosome and the number of THs in each chromosome ranging from one (Chr 14) to six (Chr 2). The 40 CsTH proteins ranged from 192 (CsTH24) to 734 (CsTH15) in length with molecular weights (MW) that varied from 21.66 to 82.12 kDa, and isoelectric point (pI) ranges from 4.5 (CsTH10) to 10.54 (CsTH14). In addition, 30 CsTH proteins were predicted to be located in the nucleus, suggesting their function of transcriptional regulation; five were located in chloroplast, two were located in the cytoplasm, and three CsTHs were located in the mitochondrion, Golgi apparatus, and cell wall, respectively (Table S1).

2.2. The Phylogenetic Relationship and Protein Structure Analysis of CsTHs

To explore the phylogenetic relationships of the TH proteins among different species, 126 TH proteins from *C. sinensis*, *Arabidopsis*, and *P. trichocarpa* were used for constructing a phylogenetic tree. The phylogenetic analysis showed that all of these CsTHs could be divided into five classes, with each category containing five in the GT1 subfamily, eight in the GT2 subfamily, two in the GT γ subfamily, seven in the SH4 subfamily, and 18 in SIP1 subfamily, respectively (Figure 1). Exon/intron structure analysis showed that 40 CsTHs contain one to 16 exons. 14 CsTHs lack introns, with 12 in the SIP subfamily and two in the GT γ subfamily. In the GT2 subfamily, five of eight TH genes contained three exons. A motif analysis of the CsTH proteins was obtained with the MEME program, and the results showed that most CsTH proteins had motifs 1, 2, 4, and 5, which correspond to the MYB_DNA-binding domain. Motifs 3 and 6 correspond to the ASIL1/2-like (IPR044823) domain and are mainly presented in the SIP subfamily. Intron/Exon analysis showed that most genes in the SIP1 and GT γ subfamilies only contained one exon, while GT2 and SH4 subfamilies had one intron (Figure 2). Additionally, we found that the genes in the GT1 subfamilies contained more introns than those in the other subfamily. The results indicate that most genes clustered in the identical subfamily showed similar exon/intron structures and arrangements, indicating that the functions of the trihelix proteins in each defined subfamily may be similar.

2.3. The Chromosome Distribution and Synteny Analysis of the Trihelix Gene in *C. sinensis*

To better understand the mechanism of the genomic distribution of CsTHs on *C. sinensis* chromosomes, a chromosome map of CsTHs was constructed based on the genomic sequences of *C. sinensis*. The results showed that all CsTHs were located on the *C. sinensis* chromosomes; Chr 2 contained the most TH members, none of which were on Chr 4 and Chr 7 (Figure S1). We performed further research on 40 CsTHs located on chromosomes and found 15 possible pairs of duplicated genes. According to the results of the gene repetition analysis, all identified paralogous genes were segmental duplications, with no tandem duplication of CsTHs in any chromosomes. This indicates that segmental duplication is the primary expansion mechanism of the CsTH gene family. TB tools calculated Ka/Ks (synonymous/non-synonymous) values, and the ratio of Ka/Ks varied from 0.193 to 0.588,

indicating that purifying selection plays a vital role during gene replication (Supplementary Table S2).

We also investigated the TH homologous gene pairing between different species to explore the species' evolutionary relationships. Dual synteny analysis revealed that these species also exhibited homology. For example, 20 CsTHs and 19 AtTHs were orthologous gene pairs, resulting in 29 syntenic relationships between *C. sinensis* and *Arabidopsis*. Six OsTHs and 10 CsTHs resulted in 13 syntenic relationships between *Oryza sativa* and *C. sinensis*. Twenty-nine CsTHs and 34 PtTHs were orthologous gene pairs, resulting in 61 syntenic relationships between *C. sinensis* and *P. trichocarpa* (Figure 3). These results propose that TH genes possessed a degree of homology in different species; *C. sinensis* and *P. trichocarpa* exhibited the highest level of homology.

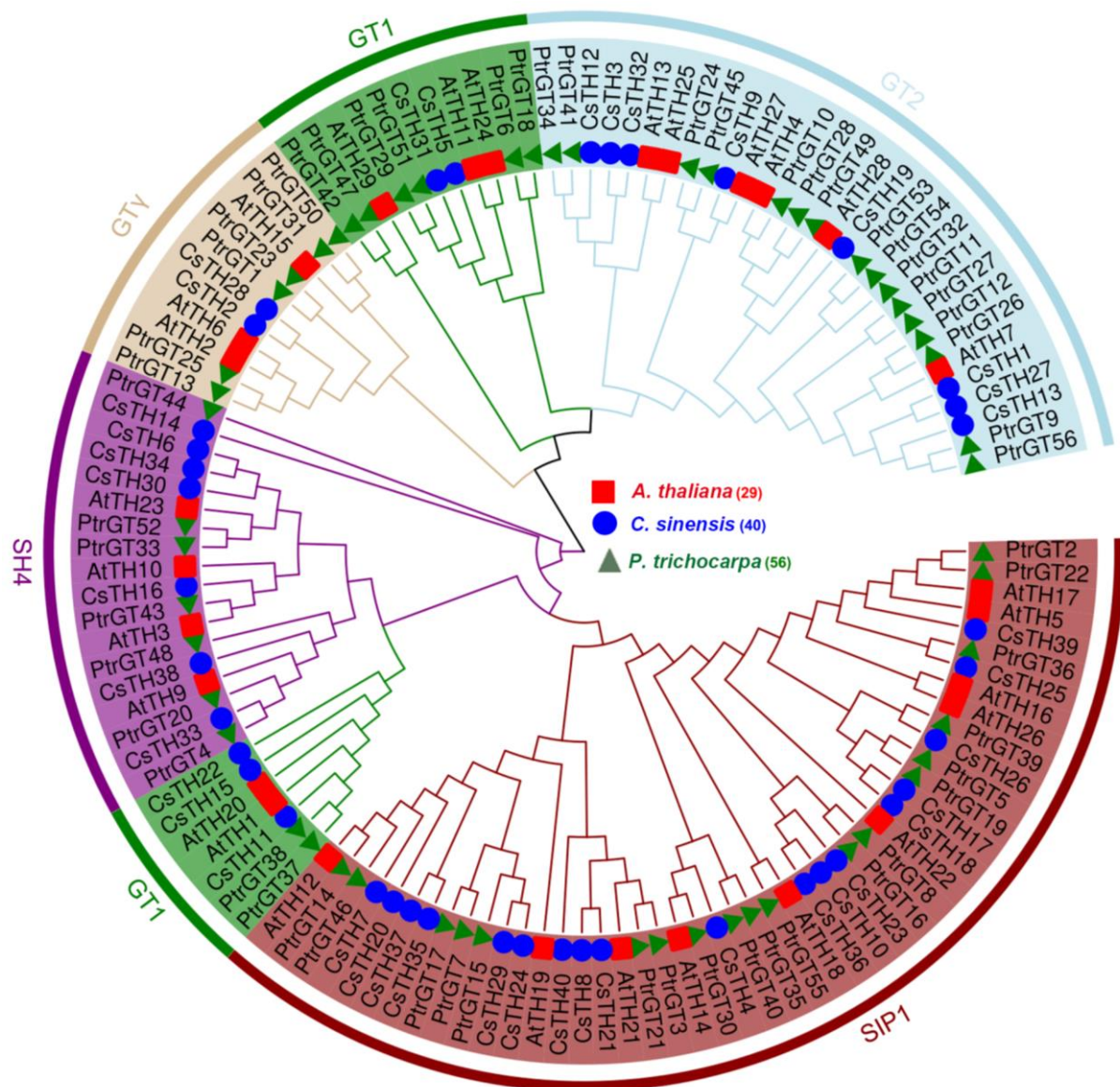


Figure 1. Phylogenetic analysis among 125 trihelix proteins in *Arabidopsis thaliana*, *P. trichocarpa*, and *C. sinensis*. The different colors represent the subfamilies of the trihelix proteins. The trihelix proteins of *Arabidopsis thaliana*, *P. trichocarpa*, and *C. sinensis* are marked with red squares, blue circles, and green triangles, respectively.

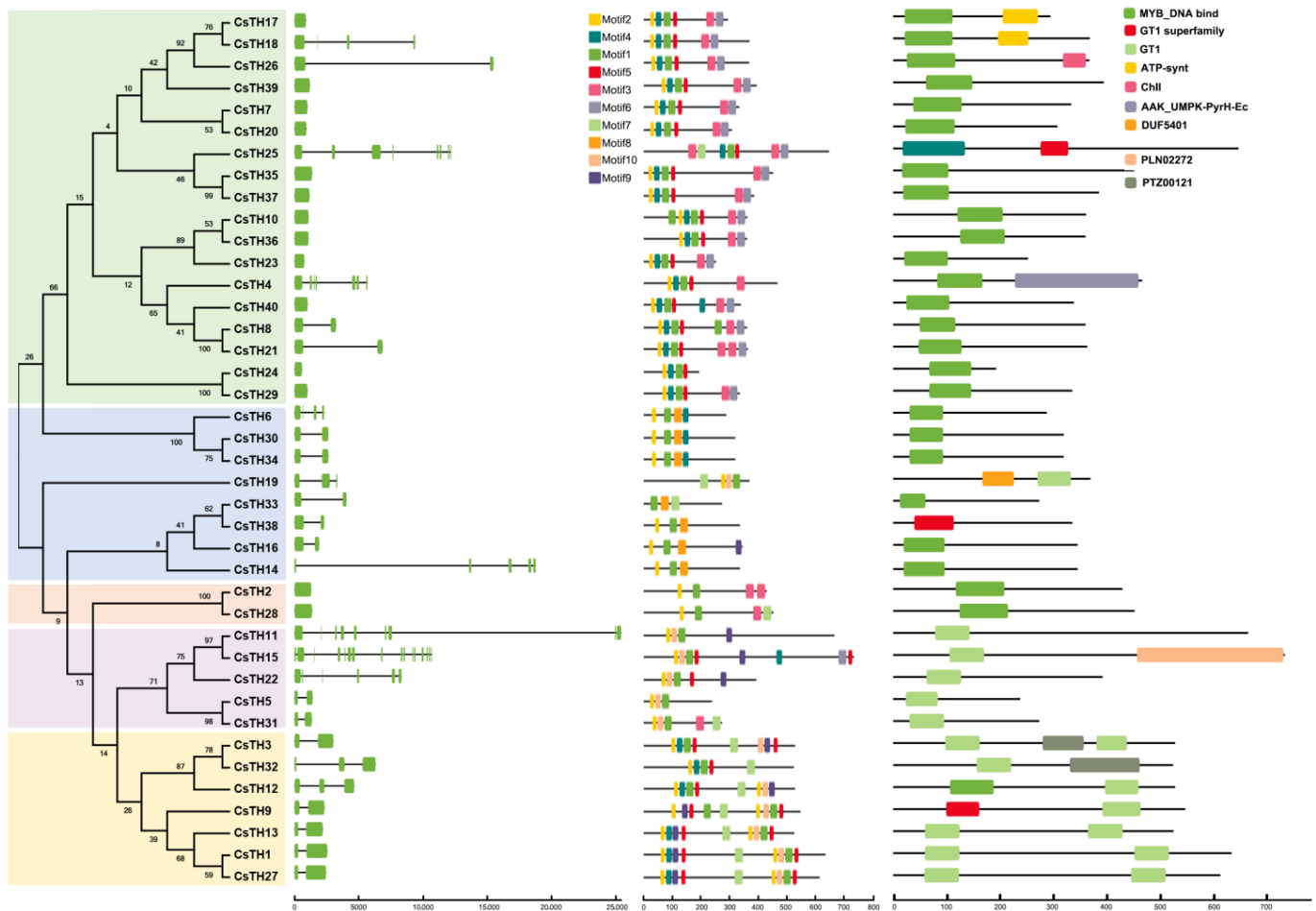


Figure 2. Gene structure, motif compositions, and conserved regions of the trihelix genes in *C. Sinensis*. Exon and intron structures of THs are graphically represented by orange boxes and black lines, respectively. The protein sequences of THs are used to predict the conserved regions and motifs. Conserved motifs are indicated by a colored box numbered 1 to 10.

2.4. The Promoter Analysis for the CsTH Gene Family

In the promoter analysis, two categories of cis-elements were discovered in the 35 CsTH genes. The first category is plant hormone response elements. The number of methyl jasmonate (MeJA)-responsive elements (TGACG-motif/CGTCA-motif) amounts to 120, with an average of three per gene. ABA-responsive elements (ABRE) and ethylene-responsive elements (ERE) come second and third at 84 and 80, with two per gene. By comparison, gibberellin-response elements (GARE, TATC-box, and P-box), Auxin (AuxRR-core and the TGA element), and salicylic acid-responsive elements do not have as many as they do, despite more kinds of motifs. The second category is abiotic and biotic stress-response elements. The anaerobic induction regulatory element (ARE) has the largest number of 76 in total, with an average of 1.9 per gene, and the light-responsive element (G-box), followed by a number of 69. In addition, the number of low temperatures (LTR and C-repeat/DRE), the Wound-responsive element (WUN-motif), defense and stress (TC-rich repeats), as well as drought (MBS)-responsive elements accounted for 35, 32, 20, and 15, respectively (Figure 4A). For the same kind of regulatory elements, it presents preference as codons for THs. The proportion of CGTCA and TGACG element components is similar in Methyl Jasmonate elements. The P-box motif has the largest number as compared to the TATC-box and the GARE-motif for gibberellin-responsive elements. The TGA element has much more than the AuxRR-core element. In low-temperature elements, the LTR element is more than the C-repeat/DRE element (Figure 4B). The detection of these cis-acting ele-

ments suggested that the CsTHs can respond to a variety of hormones and stresses, and these response elements may directly affect the stress response ability of CsTHs under stress conditions.

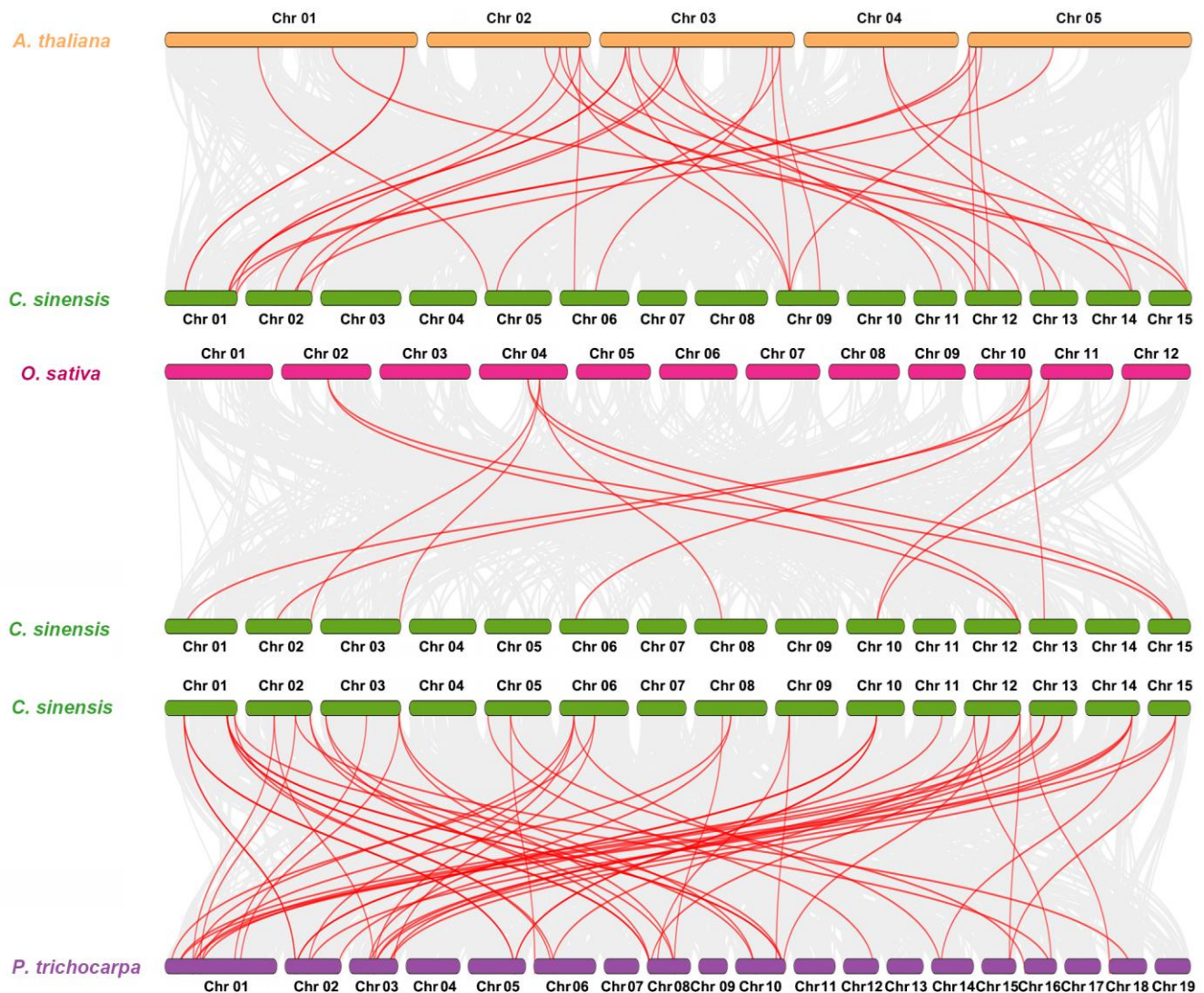


Figure 3. Synteny analysis of TH genes between *C. sinensis* and three representative species. Red lines highlight the orthologous TH gene pairs between *C. sinensis* and other plant genomes, while the gray lines in the background indicate the collinear blocks.

2.5. The Tissue and Organ Expression Pattern of CsTHs in the Tea Plant

Gene expression patterns can provide helpful information about the physiological functions of CsTHs. The expression profiles covering eight tissues in the tea plant were analyzed using the publicly available RNA-seq dataset released in TPIA to estimate the physiological roles of 40 CsTH genes. The heat map visualized the relative expression of 40 CsTHs and showed a wide range of expressions, and these genes could be grouped into three primary categories. The first expression pattern showed that all CsTHs, except for CsTH33 in the SH4 group, CsTH12, and CsTH22, were extremely low in all of the examined tissues. Compared with these, 14 CsTHs in SIP1, three CsTHs in GT2, and one CsTH gene each in GT1 and GT γ were constitutively expressed with high levels in all the tissues, with some genes displaying high expression levels in specific tissues such as the following: CsTH7 and CsTH20 high expression in the root, and CsTH8 and CsTH21 high expression in the stem. The remaining genes that made up the final expression pattern

were also constitutively expressed in all tissues but at low levels (Figure 5). Most CsTHs in the same subfamily displayed similar expression patterns, whereas the CsTHs in different subfamilies were diverse. Based on tissue-specific expression, eight representative CsTHs from four subfamilies were subsequently investigated in other tissues of the tea plant cultivar (Longjing43) utilizing qRT-PCR (quantitative real-time polymerase chain reaction) analyses (Figure 6). The expression patterns of these CsTHs were highly consistent with their transcriptomic profiles from RNA-seq.

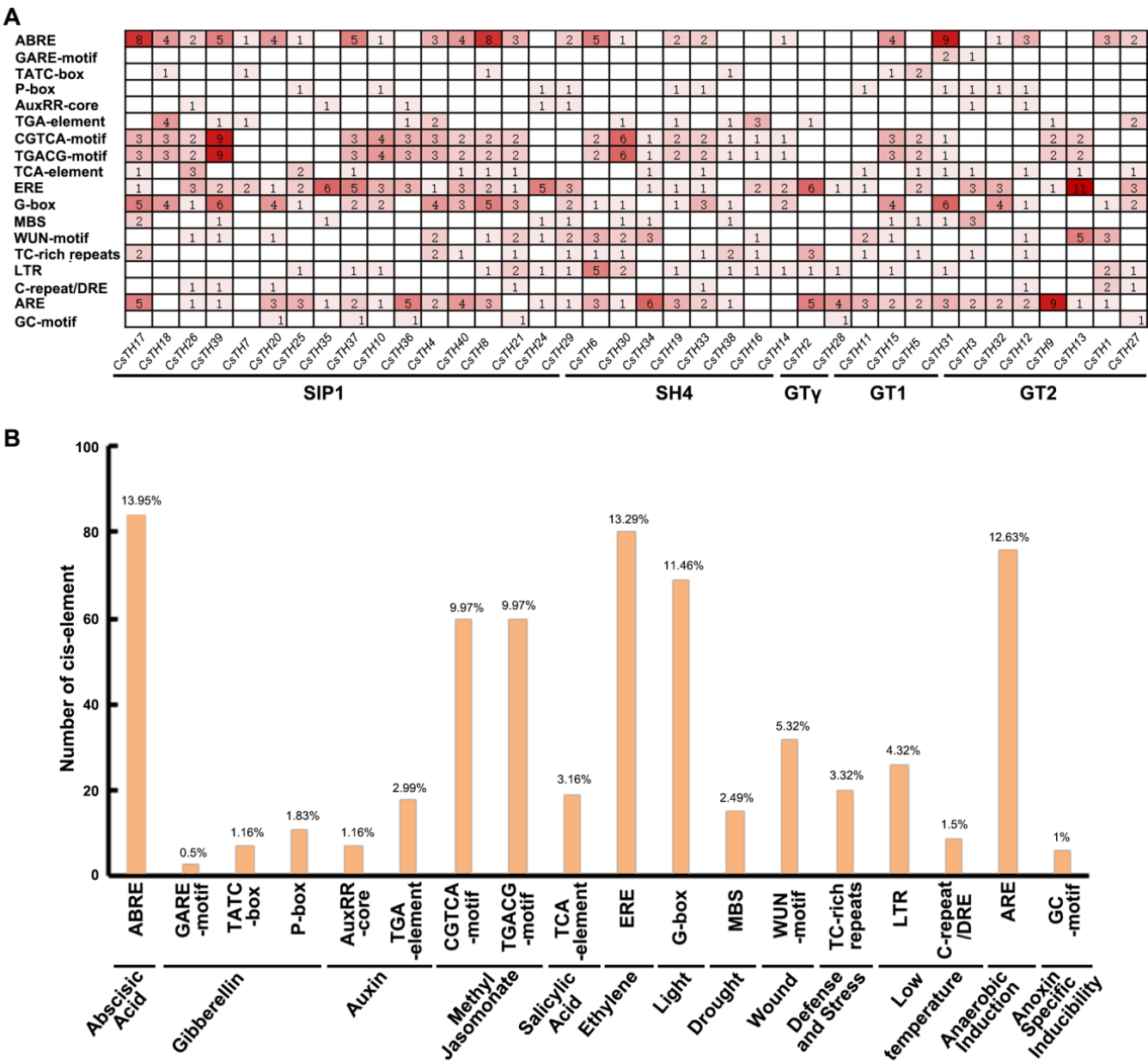


Figure 4. (A) These numbers indicate the total number of cis-elements for each CsTH gene. (B) The categorization of cis-acting elements relevant to abiotic stresses and plant hormone responses. The percentages and quantities of factors in each category are presented.

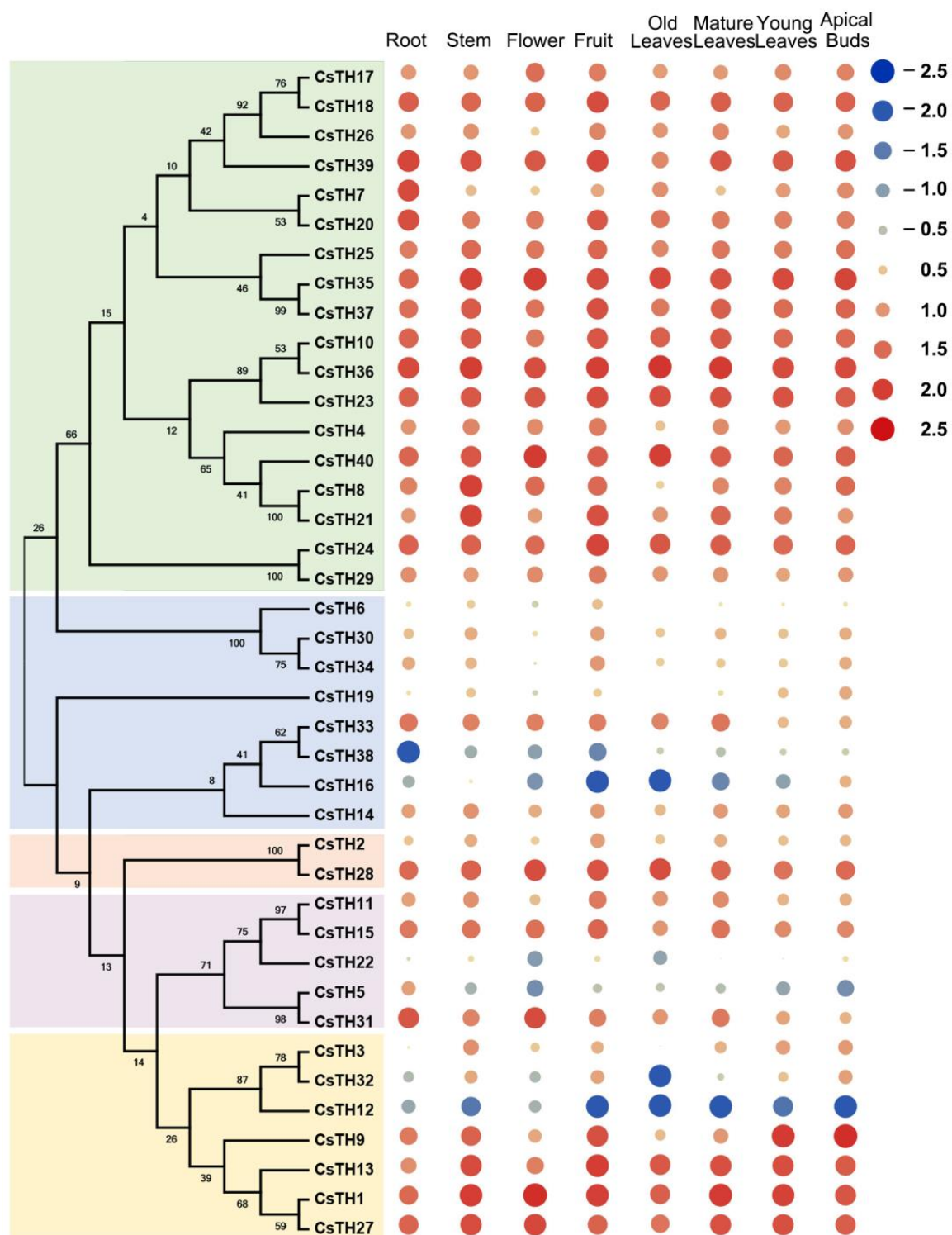


Figure 5. The expression patterns of CsTHs genes in the root, stem, old leaf, flower, fruit, mature leaf, young leaf, and apical bud of the tea plant were calculated using $\text{Log}_{10}(\text{FPKM})$. Most of the data were distributed between -2.5 and $+2.5$, the color and size of the dots represent expression levels. Blue dots and red dots are indicated low and high expression levels, respectively.

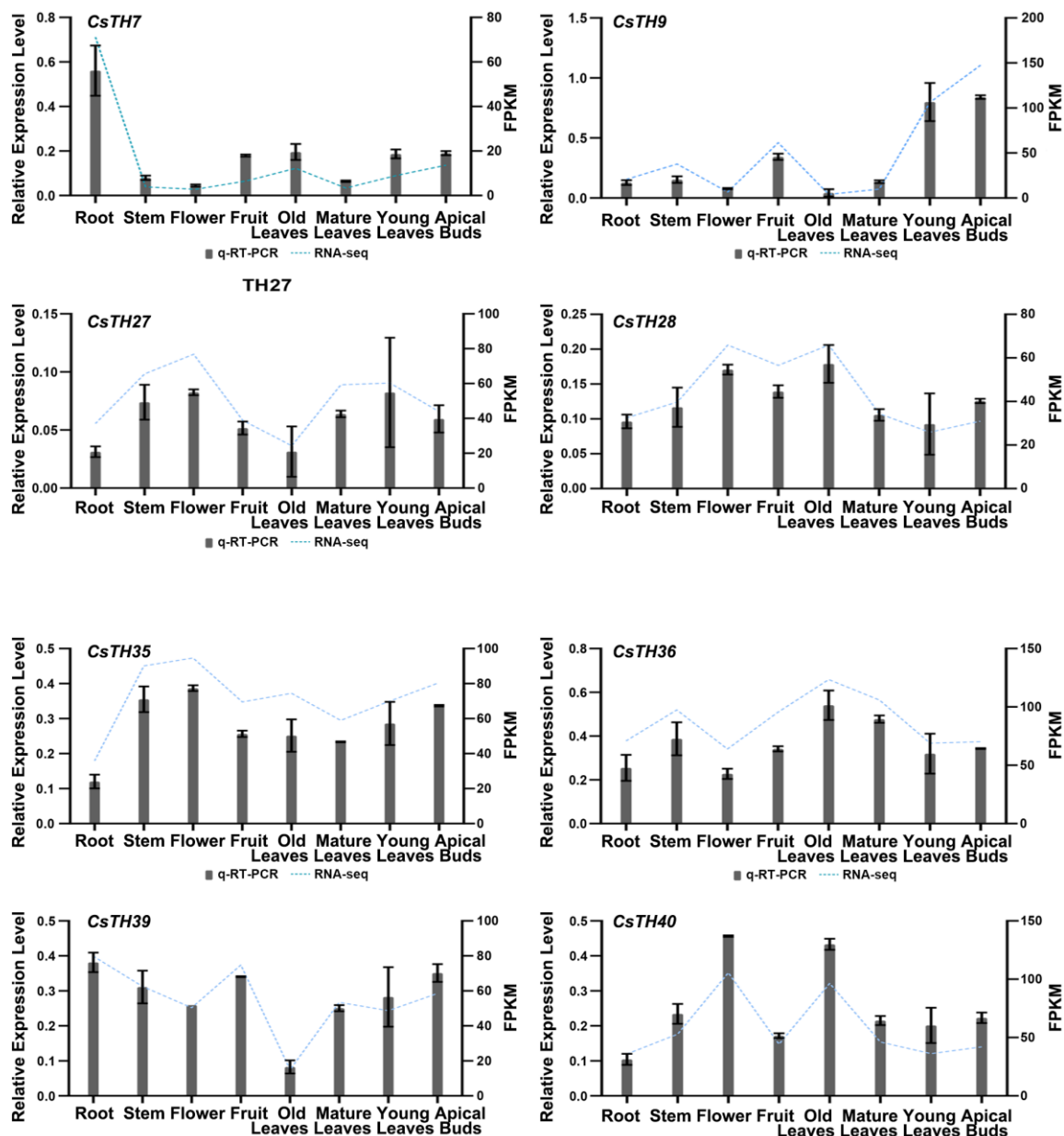


Figure 6. Real-time qRT-PCR analysis of eight TH genes in different tissues in tea plants. Error bars indicate the SD of three biological replicates.

2.6. The Expression Profiles of CsTHs in Response to Abiotic Stress

High salt and drought stress accelerate the accumulation of ABA in plants, and the accumulated abscisic acid can induce the expression of ABA-responsive genes and stomatal closure in leaves, improving plant salt resistance and drought resistance [43,44]. Considering the expression of the CsTHs and the existence of ABRE elements in their promoter, we examined the expression profiles of eight CsTHs in response to ABA treatment, drought, and NaCl stress through the quantitative real-time polymerase chain reaction. The results showed that all eight CsTHs were strongly induced in response to ABA treatment and reached peak at 3 h. CsTH28 was upregulated more than fourfold. For drought stress, after three h of a PEG-6000 treatment, the expression levels of CsTH28 and CsTH39 were upregulated and gradually decreased. CsTH7 was upregulated and peaked at 6 h, while the CsTH36 and CsTH40 were gradually upregulated and peaked at 12 h. For the NaCl treatment, the expression levels of CsTH9 and CsTH27 were decreased and then gradually

increased to high levels at 12h. CsTH28 and CsTH35 expression levels remained the same at the beginning. Then, they upregulated to high levels at 12 h; CsTH36 and CsTH39 were upregulated and peaked at six h (Figure 7). The integration of expression data under multiple treatments suggested that CsTH28, CsTH36, and CsTH39 responded to drought and salt stress, and thus, we further investigated its function.

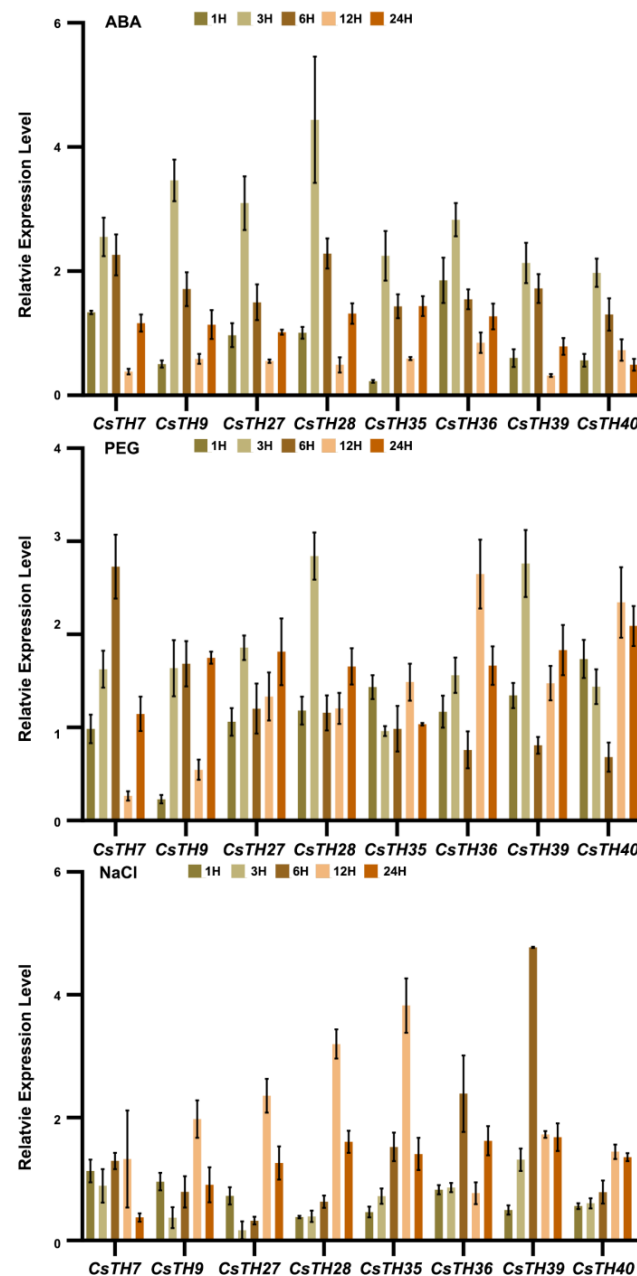


Figure 7. Expression patterns of CsTHs under ABA, PEG, and NaCl stress. Error bars indicate the SD of three biological replicates.

2.7. The Subcellular Localization and Transcriptional Activation Activities of CsTH28/36/39

The expression levels of the CsTH28/36/39 genes were relatively high with the ABA, drought, and NaCl treatments. The constructed GFP: Pcambia1300-TH28/36/39 fusion vectors and the 1300 empty vector were independently transiently transformed into tobacco (*Nicotiana benthamiana*) leaves. The protein-coding nucleotide products of CsTH28 and CsTH36 were mainly expressed in the nuclei, while CsTH39 was localized at the nuclei and cell membrane (Figure 8A).

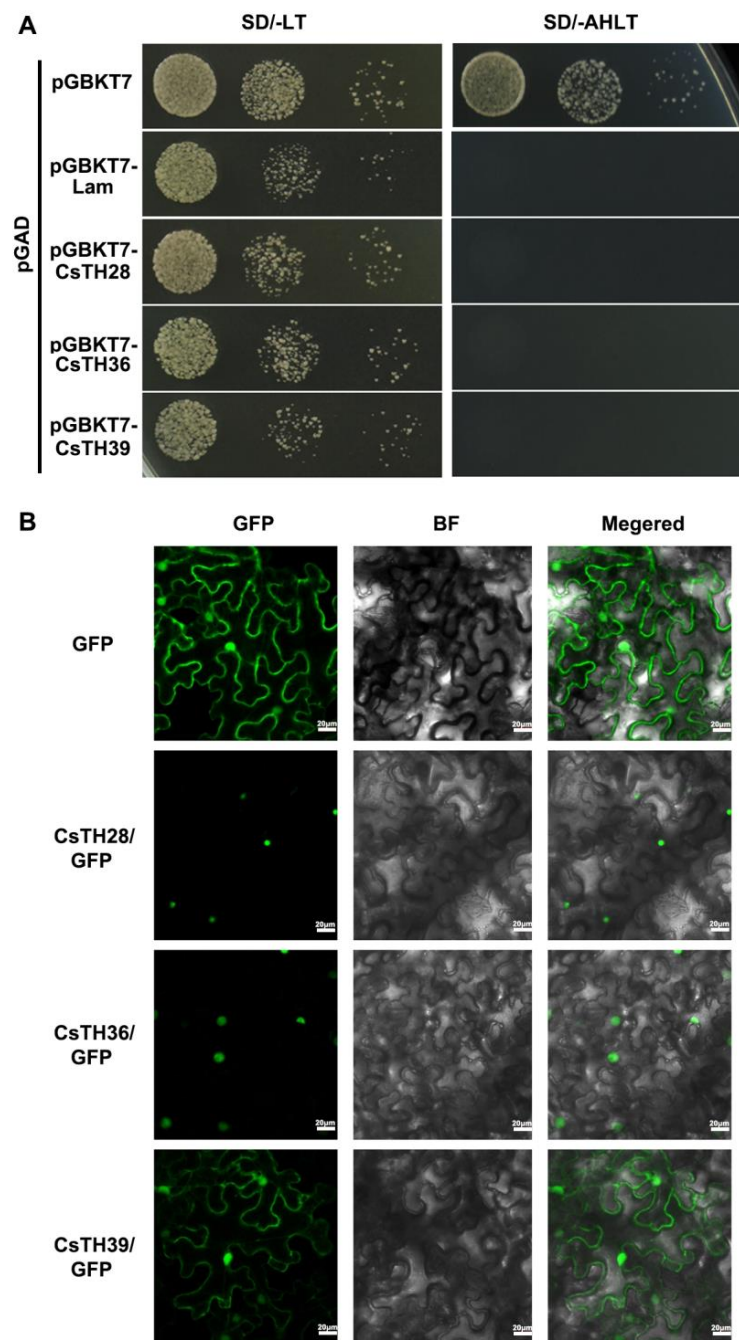


Figure 8. The potential function of CsTHs in tea plants. **(A)** Transactivation analyses of CsTH28, CsTH36, and CsTH39 in yeast. Negative control (pGBKT7-Lam) and positive control (pGBKT7-53) were transformed into the AH109 strain and successively incubated in SD/-Leu/-Trp media and an SD/-Ade/Trp/-Leu/-Trp/-His plate. **(B)** Subcellular localization of CsTH28, CsTH36, and CsTH39. GFP, CsTH28-GFP, CsTH36-GFP, and CsTH39-GFP were transiently expressed in tobacco leaves. GFP: Green fluorescence image, BF: Bright-field microscopy image, Merge: Merged bright-field and green fluorescence images.

The transcriptional activation of CsTH28/36/39 was investigated by constructing pGBK vectors that were then transformed into the yeast strain AH109. The results of transcriptional activation activity showed that CsTH28/36/39 could grow on the SD/-Leu/-Trp medium as well as negative (pGBKT7-lam) and positive (pGBKT7-53) controls. In contrast, the yeast strains transformed with the negative control pGBKT7-lam vector and

CsTH28/36/39 could not grow on the SD/-Ade/-His/-Leu/Trp medium. Only the transformants containing pGBKT7-53 can grow on an SD-Dropout-deficient medium, indicating that the full-length sequences of CsTH28/36/39 did not possess transcriptional activation activity to activate the expression of downstream reporter genes (Figure 8B).

2.8. The Function of CsTH28/36/39 in Responsive to Osmotic Stress

Transcription is crucial in long-term stress adaptation and protection against future stresses. Owing to efficient validation, yeast has enabled studies of gene regulation and biology under stress. Thus, to assess the relevance of the CsTH28/36/39 on cell growth upon osmotic, we transformed the CsTH28/36/39 into the *S. cerevisiae* (INVSc1 and BY4741) strain and monitored cellular growth in the presence of high osmolality (0.8 M NaCl and 0.8 M mannitol). The growth of the control (INVSc1 and BY4741 transformed with empty vector) and recombinant strain containing CsTH28/36/39 maintained growth on the SG/-U medium. However, wild-type cells impaired growth under high osmolality conditions (0.8 M NaCl and 0.8 M mannitol). Under salt treatment, the yeast cells overexpressing CsTH28 and CsTH39 could grow properly when the cells were diluted by 10^2 , while CsTH36 could grow normally when the cells were diluted by 10^3 . Under mannitol treatment, the yeast cells overexpressing CsTH28 and CsTH39 could grow properly when the cells were diluted by 10^4 , while CsTH36 could grow normally when the cells were diluted by 10^3 . These results show that CsTH28/36/39 could enhance the tolerance to osmotic stress, with CsTH36 conferring the highest tolerance to salt stress, while CsTH28 and CsTH39 show higher tolerance to mannitol than CsTH36 (Figure 9). These results indicated that the CsTH28/36/39 gene was involved in response to salt and drought stress in tea plants.

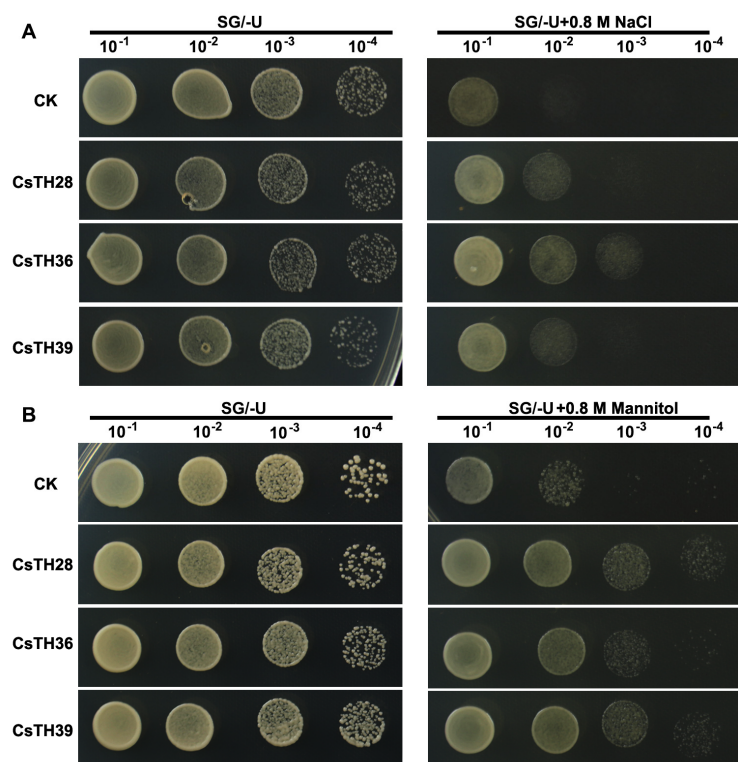


Figure 9. Overexpression of CsTHs improves osmotic stress tolerance in transgenic yeast. (A) The empty vector (CK) and the CsTHs spotted onto SG-U plates with and without 0.8 M NaCl and grown at 30 °C for 3–5 days. (B) The empty vector and the CsTHs were spotted onto SG-U plates with and without 0.8 M mannitol and grown at 30 °C for 3–5 days.

3. Discussion

Early research revealed that the GT factor family regulates morphogenetic processes and acts as a class of light regulators, which explains their roles in controlling light-responsive genes [45]. However, more recent studies have provided compelling evidence that the trihelix family also plays a significant role in plant growth and development and the responsiveness to environmental cues [27,46]. In this study, we identified 40 trihelix genes in the *C. sinensis* genome, distributed across chromosomes with varying densities. Previously, trihelix family genes were classified into three distinct subfamilies (GT α , GT β , and GT γ) [22]. However, Kaplan-Levy et al. (2012) classified trihelix genes from *Oryza sativa* and *Arabidopsis* into five clades: GT-1, GT-2, SH4, SIP1, and GT γ . Recently, a new subfamily, GT δ , was identified in tomato and rice [11,47]. Phylogenetic analysis demonstrated that 40 CsTHs were divided into five subfamilies, with subfamily members sharing similar gene structures and motif distributions, implying that these genes may have shared a common ancestor and similar functions. Furthermore, at least one CsTH protein was detected in each subgroup of AtTH and PtTH proteins, indicating that the differentiation of the trihelix TF family occurred prior to the divergence between monocots and dicots.

The similarity in gene structures and motif distributions among subfamily members suggests that they may have originated from gene duplication events. Fifteen segment duplication events were identified among 40 CsTHs, which supports this hypothesis. Furthermore, a group of CsTHs was linked to numerous syntenic gene pairs, suggesting that these genes may play a significant role in the evolution of the trihelix gene family and were essential for plant development and defense mechanisms. All segmental duplication events in the *C. sinensis* gene trihelix family occurred during a recent whole genome duplication event. The duplicated genes that experience sub-functionalization through purifying selective pressure ($K_a/K_s < 1$), neo-functionalization through positive selective pressure ($K_a/K_s > 1$), and non-functionalization play essential roles in adaptive evolution. In this study, all of the K_a/K_s ratios in the different trihelix gene pairs are less than one, suggesting that all the duplicated genes experience a strong purifying selective pressure and are sub-functionalized during evolution. This phenomenon is consistent with the fact that most duplicated genes are sub-functionalized in *C. sinensis*. Additionally, gene synteny analyses showed that most CsTH genes displayed syntenic relationships with those in *Arabidopsis* and *populus*. Conversely, there are fewer collinearity gene pairs with monocotyledonous plants, with only 13 gene pairs with rice. This suggests that some redundant TH genes were lost during evolution.

Light plays a crucial role in influencing tea leaf quality. Early research focused on the role of GT factors in regulating gene expression in response to light [48,49]. However, subsequent studies revealed that these genes also contribute to plants' responses to salt, drought, and hormone signaling [11,50]. The cotton gene Gh_A05G2067 shows increased expression under drought and salt stress [51]. Similarly, the tomato GT-1 gene ShCIGT displays increased expression under drought and low-temperature stress [20]. Upstream regulatory factors can regulate the expression levels of target genes by recognizing and binding to cis-acting elements located on the promoter region. These regulatory elements, in turn, govern various biological processes. Over the years, the functions and pathways associated with many cis-acting elements have been deciphered. An analysis of the promoter sequences of TH genes in *C. sinensis* revealed a significant abundance of hormone- and stress-responsive elements. Plant hormones are organic compounds produced in trace amounts within plants, and they play a crucial role in regulating various physiological processes throughout their life cycle. Abscisic acid (ABA), commonly referred to as a stress hormone, regulates stomatal opening, growth, and development, but also contributes to plant responses to abiotic stress [52,53]. By conducting qRT-PCR, we observed that all of the selected genes were regulated by ABA treatment. Our focus on the expression of the eight TH genes mentioned above revealed that CsTH28, CsTH36, and CsTH39 exhibited distinct responses to drought and salt treatment. These three CsTH genes could be promising candidates for further investigations into abiotic stress tolerance in *C. sinensis*.

Because transcription factors have nuclear localization signal (NLS) regions, most transcription factors are localized within the nucleus. However, there are exceptions such as AtHSFA6a, which resides in the cytoplasm, and TaMIF4-5D, which is found both in the nucleus and cell membrane [54,55]. We identified CsTH28 and CsTH29 as nuclear-localized genes. This observation suggests that these two genes may function as transcription factors. However, some transcription factors exhibit dual localization, meaning that they are present both in the nucleus and the cell membrane. Previous studies have demonstrated the intricate roles of transcription factors in plant stress responses. Under salt stress, the NAC (NAM, ATAF and CUC) transcription factor AtNLT8 translocates from the cytoplasm to the nucleus, activating downstream stress resistance genes and enhancing plant tolerance [56,57]. Similarly, the TaNLT1 transcription factor rapidly shuttles between the plasma membrane and the nucleus under drought stress, relaying signals to activate early response genes [58]. AtNLT8 and TaNLT1 contain transmembrane motifs, and both are released from the membranes by proteolytic cleavage, possibly in response to stress conditions, and transported into the nucleus where they regulate the expression of stress responsive genes. Comparatively, drought treatment triggers the expression of the OsFTIP6-OsHB22-OsMYBR57 module. OsFTIP6 (FT-INTERACTING PROTEIN6) interacts with OsHB22, promoting its nucleocytoplasmic shuttling, where it further interacts with OsMYBR57 to directly activate OsbZIPs (basic leucine zipper), enhancing drought tolerance in rice [59]. We performed transmembrane domain prediction analysis on CsTH39 and found that it does not contain transmembrane domain. Our findings regarding CsTH39's location in both the nucleus and cell membrane and its precise localization and response to osmotic stress warrant further in-depth investigation. The transcriptional auto-activation experiment using yeast two-hybrid assay revealed that none of the CsTH genes exhibited auto-activation activity. It is speculated that the proteins of the CsTH family may regulate gene expression or participate in different physiological functions by forming homotypic or heterodimers.

Drought and salinity, as major environmental abiotic stresses, negatively impact crop development, yield, and quality. It is well-known that osmotic stress response mechanisms involve several particular physiological and biochemical pathways that allow Persian walnut to adapt to unfavorable conditions [60]. The regulatory roles of certain TH genes in salt and drought responses have been reported. In soybean plants, the transgenic GmGT-2B and GmGT2A plants enhance salt tolerance, frost resistance, and drought resistance, and they respond to ABA [30]. Trihelix transcription factors play a role in *Arabidopsis* by influencing embryonic development and the plant's response to drought and salt stress [61,62]. Among the multitude of genes involved in various abiotic stress responses in rice, OsGT γ -1, and SHA1 stand out as compelling examples: overexpression of OsGT γ -1 bolsters salt stress tolerance in rice seedlings, whereas mutations in SHA1 lead to delayed abscission of rice seeds [11,22,63]. The overexpression of the wheat trihelix gene TaGT2L1D in *Arabidopsis* increased the number of stomata in *Arabidopsis* leaves and decreased the drought tolerance of the plants [29]. Under abiotic stress conditions, yeast will initiate stress responses and regulate gene expression to enhance stress resistance. At present, many studies have performed antistress gene phenotypic validations through yeast due to the fact that the validation procedure is simple, efficient, and has wide applications [64–66]. We made a preliminary exploration of the function of CsTH genes in response to osmotic stress in yeast. Consistent with findings in other species, the overexpression of CsTH28/36/39 in yeast strains increased tolerance to osmotic stress. These data suggest that CsTH28/36/39 might play a crucial role in osmotic stress response and pave the way for further investigations.

4. Materials and Methods

4.1. Identification of CsTH genes in the *C. sinensis* Genome

The previously reported TH-encoded proteins from *Arabidopsis* [67] and *P. trichocarpa* [12] have close phylogenetic relationships with the tea plant. Genewise v2.2.0 software [68] was used to search the TH sequence from the tea plant genome sequence using amino acid sequences

from *Arabidopsis* and *P. trichocarpa*. The Pfam database (<http://pfam.sanger.ac.uk>, accessed on 1 September 2023) was used to analyze the Hidden Markov model (HMM) of the selected CsTHs. SMART (<http://smart.embl-heidelberg.de/>, accessed on 3 September 2023) and the NCBI Conserved Domain Database (<http://www.ncbi.nlm.nih.gov/Structure/cdd/wrpsb.cgi>, accessed on 4 September 2023) were used to filter the redundant sequences and confirmed all the potential CsTH genes (for the existence and integrity of the TH domain and domain). ExPASy was used to predict the isoelectric point (pI), molecular weight (MW), and grand average of hydropathicity (GRAVY). WoLF PSORT was used to predict the subcellular localization of the CsTH proteins.

4.2. Conserved Motifs, Gene Structure, Promoters, and Evolutionary Analyses of the THs

The TH protein sequences from *Arabidopsis*, *P. trichocarpa*, and *C. sinensis* were aligned using the ClustalX 1.83 program. Phylogenetic trees for three species of TH protein sequences were constructed by MEGA 6.0 software using the NJ (Neighbor-Joining) method with the following parameters: the bootstrap method (1000 replicates), the Poisson model, uniform rates, and complete deletion. The motif of CsTHs was conducted on the MEME website (<http://meme-suite.org/tools/meme>, accessed on 5 September 2023) with the maximum number of motifs set as 10. The intron and exon were displayed by the online website gene structure display server (GSDS 2.0, <http://gsds.cbi.pku.edu.cn>, accessed on 5 September 2023). Cis-acting regulatory elements were annotated using an online tool (<http://bioinformatics.psb.ugent.be/webtools/plantcare/html/>, accessed on 8 September 2023). The basic characteristic data about the TH proteins were calculated using the program tool (<http://web.expasy.org/protparam/>, accessed on 8 September 2023). The secondary structures of the proteins were analyzed using a scratch protein predictor (<http://scratch.proteomics.ics.uci.edu/>, accessed on 10 September 2023).

4.3. Analyses of Synteny

The CsTH genes' physical position in the *C. sinensis* genome database was established by Tbtools. The CsTH gene duplication events were examined by MCScanX software (University of Georgia, Athens, GA, USA) with default parameters. The matching genes were drawn by the Circos-0.67 program to visualize the duplicated regions in the *C. sinensis* genome (<http://circos.ca/>, accessed on 11 September 2023). The homology of the TH genes between *C. sinensis* and the other species (*Arabidopsis*, *O. sativa*, *P. trichocarpa*) was analyzed by a dual synteny plotter of Tbtools [69].

4.4. TH Transcription Factors Expression Pattern in *C. sinensis*

The expression pattern data of eight tissues and four kinds of abiotic stress, including root, stem, old leaf, mature leaf, young leaf, apical bud, flower, and fruit, as well as cold, PEG, MeJA, and NaCl stress treatments, were downloaded from the Tea Plant Information Archive (TPIA). The expression level of the TH genes was displayed as Log10 FPKM (fragments per kilobase of exon per million fragments value) in a heat map using the Mev4.9.0 software. The ABA and PEG treatments were documented according to a previous report [41]. An amount of 100 µM ABA was used to spray the tea plant leaves for ABA treatments (ddH₂O as control). For drought treatments, 20% PEG was rinsed into the tea plant roots (ddH₂O as mock control). The primers for CsTHs were designed by Beacon Designer 7.0 software. Glyceraldehyde-3-phosphate dehydrogenase (GAPDH, accession number: KA295375.1) was used as an internal reference. The real-time PCR on an ABI7900HT sequence detection system was found by using SYBR Green (Applied Biosystems, Waltham, MA, USA).

4.5. RNA Extraction and qRT-PCR Analysis

According to the manufacturer's instructions, the total RNA was extracted from plant materials using an RNAPrep Pure Plant Kit. The first-strand cDNA was synthesized from the total RNA using a PrimeScript RT reagent kit according to the manufacturer's

instructions—the program and reaction system of qRT-PCR as per the previously reported protocol. The *CsGAPDH* gene was selected as the internal control. All specific primers are listed in Table S3. In different cases, the relative gene expression was quantified using $2^{-\Delta\text{CT}}$ methods.

4.6. Transcriptional Self-Activating of CsTHs Proteins

The pGBK-CsTHs and pGBK constructs were transformed into the yeast strain AH109, and the transformants were inoculated on an SD/-Trp medium. Further, the colonies were transferred to an SD/-His/-Leu/-Trp medium and incubated at 30 °C for 3–5 days.

4.7. Subcellular Localization of CsTHs Proteins

The CsTHs without stop codons were amplified using primers with homologous arms and appropriate enzyme digestion sites (BamH I) before being cloned into the pCambia1300-35S-EGFP vector using the 2× Ezmax[®] Universal CloneMix (Tolo Biotech., Shanghai, China). This allowed the CsTH genes to fuse with the GFP protein driven by the 35S promoter when expressed in tobacco (*N. benthamiana*) leaves. Two days after infiltration, the expression of GFP in tobacco leaves was examined using a Leica TCS SP5 confocal laser scanning microscope (Leica Microsystems, Bannockburn, IL, USA) 44–48 h after infiltration.

4.8. Validation of Gene Function in Yeast

pYES2 is a high-copy-number plasmid vector that leverages the potent, galactose-inducible GAL promoter system to allow tightly regulated, high-level gene and protein expressions in yeast. It contains supporting elements like the *ura3* marker for transformant selection [70]. The full-length coding sequences of CsTHs were amplified by PCR to generate pYES2-CsTHs yeast expression vectors using the 2× Ezmax[®] Universal CloneMix (Tolo Biotech.). The pYES2 vector was linearized by digestion, using the restriction enzymes KpnI and BamHI. INVSc1 and BY4741 are well-suited hosts for heterologous protein expression due to their capacity to carry out post-translational modifications on translated proteins [66,71]. pYES2 and pYES2-CsTHs plasmids were transformed into INVSc1 and BY4741 by the lithium acetate method. These yeasts were plated on an SD/-U medium and validated by PCR after three days of incubation at 30 °C. Subsequently, the transformed INVSc1 yeast and BY4741 yeast were spotted onto the SG/-U medium with 0.8 M NaCl and 0.8 M mannitol, respectively.

4.9. Statistical Analysis

All experiments were carried out with at least three independent biological replicates. Each measurement was carried out in triplicate. Data represent the mean \pm sd of three biological replicates.

5. Conclusions

In conclusion, 40 members of the trihelix gene family were identified in the *C. sinensis* genome and were classified into five subfamilies based on phylogenetic relationships. Members of the same trihelix gene subfamilies share similar gene structures and conserved functional domains. All the identified segmentally duplicated gene pairs underwent strong purifying selections over evolutionary timescales. The differential expression profiles of trihelix genes under high salt stress and PEG treatments revealed three candidate genes for further investigating the stress tolerance mechanisms in *C. sinensis*. In conclusion, the present study furnishes a solid foundation for future investigations to elucidate the intricate functions and molecular mechanisms of trihelix genes, advancing our understanding of their roles in plant growth, development, and stress tolerance.

Supplementary Materials: The following supporting information can be downloaded at: <https://www.mdpi.com/article/10.3390/plants13010070/s1>, Figure S1: Distribution of 40 CsTH genes on 15 chromosomes.; Table S1: Genome-wide bioinformatics analysis of Trihelix genes in *C. sinensis*; Table S2: Ka/Ks value for duplicate trihelix genes in *C. sinensis*; Table S3: Oligonucleotide primer sequences.

Author Contributions: Z.L., Z.X. and X.Z. designed the research and performed most of the experiments; L.L., Y.H., Y.Z. and C.Z. performed some of the experiments; Z.L. and G.H. were responsible for data analysis and the writing of the manuscript. All authors have read and agreed to the published version of the manuscript.

Funding: This work was funded by the Major Science and Technology Special Project of Variety Breeding of Zhejiang Province (2021C02067-7), the Zhejiang Provincial Natural Science Foundation of China under Grant No. LQ23C020003, the National Natural Science Foundation of China under Grant No. 32272553, and the State Key Laboratory for Managing Biotic and Chemical Threats to the Quality and Safety of Agro-Products under Grant No. 2021DG700024-KF202102.

Data Availability Statement: All datasets presented in this study are included in the article/Supplementary Tables.

Conflicts of Interest: The authors declare no conflict of interest.

References

- Kaplan-Levy, R.N.; Brewer, P.B.; Quon, T.; Smyth, D.R. The trihelix family of transcription factors--light, stress and development. *Trends Plant Sci.* **2012**, *17*, 163–171. [\[CrossRef\]](#)
- Green, P.J.; Kay, S.A.; Chua, N.H. Sequence-specific interactions of a pea nuclear factor with light-responsive elements upstream of the *rbcS-3A* gene. *EMBO J.* **1987**, *6*, 2543–2549. [\[CrossRef\]](#)
- Luo, J.L.; Zhao, N.; Lu, C.M. [Plant Trihelix transcription factors family]. *Yi Chuan* **2012**, *34*, 1551–1560. [\[CrossRef\]](#)
- Qin, Y.; Ma, X.; Yu, G.; Wang, Q.; Wang, L.; Kong, L.; Kim, W.; Wang, H.W. Evolutionary history of trihelix family and their functional diversification. *DNA Res.* **2014**, *21*, 499–510. [\[CrossRef\]](#)
- Lam, E. Domain analysis of the plant DNA-binding protein GT1a: Requirement of four putative alpha-helices for DNA binding and identification of a novel oligomerization region. *Mol. Cell. Biol.* **1995**, *15*, 1014–1020. [\[CrossRef\]](#)
- Dehesh, K.; Bruce, W.B.; Quail, P.H. A trans-acting factor that binds to a GT-motif in a phytochrome gene promoter. *Science* **1990**, *250*, 1397–1399. [\[CrossRef\]](#)
- Le Gourrierc, J.; Li, Y.F.; Zhou, D.X. Transcriptional activation by Arabidopsis GT-1 may be through interaction with TFIID-TBP-TATA complex. *Plant J.* **1999**, *18*, 663–668. [\[CrossRef\]](#) [\[PubMed\]](#)
- Zhou, D.X. Regulatory mechanism of plant gene transcription by GT-elements and GT-factors. *Trends Plant Sci.* **1999**, *4*, 210–214. [\[CrossRef\]](#) [\[PubMed\]](#)
- Kuhn, R.M.; Caspar, T.; Dehesh, K.; Quail, P.H. DNA binding factor GT-2 from Arabidopsis. *Plant Mol. Biol.* **1993**, *23*, 337–348. [\[CrossRef\]](#) [\[PubMed\]](#)
- Yasmeen, E.; Riaz, M.; Sultan, S.; Azeem, F.; Abbas, A.; Riaz, K.; Ali, M.A. GENOME-WIDE ANALYSIS OF TRIHELIX TRANSCRIPTION FACTOR GENE FAMILY IN Arabidopsis thaliana. *Pak. J. Agric. Sci.* **2016**, *53*, 439–448. [\[CrossRef\]](#)
- Li, J.; Zhang, M.; Sun, J.; Mao, X.; Wang, J.; Wang, J.; Liu, H.; Zheng, H.; Zhen, Z.; Zhao, H.; et al. Genome-Wide Characterization and Identification of Trihelix Transcription Factor and Expression Profiling in Response to Abiotic Stresses in Rice (*Oryza sativa* L.). *Int. J. Mol. Sci.* **2019**, *20*, 251. [\[CrossRef\]](#)
- Wang, Z.; Liu, Q.; Wang, H.; Zhang, H.; Xu, X.; Li, C.; Yang, C. Comprehensive analysis of trihelix genes and their expression under biotic and abiotic stresses in *Populus trichocarpa*. *Sci. Rep.* **2016**, *6*, 36274. [\[CrossRef\]](#)
- Li, K.; Duan, L.; Zhang, Y.; Shi, M.; Chen, S.; Yang, M.; Ding, Y.; Peng, Y.; Dong, Y.; Yang, H.; et al. Genome-wide identification and expression profile analysis of trihelix transcription factor family genes in response to abiotic stress in sorghum [*Sorghum bicolor* (L.) Moench]. *BMC Genom.* **2021**, *22*, 738. [\[CrossRef\]](#)
- Zhao, D.; Gao, F.; Guan, P.; Gao, J.; Guo, Z.; Guo, J.; Cui, H.; Li, Y.; Zhang, G.; Li, Z.; et al. Identification and analysis of differentially expressed trihelix genes in maize (*Zea mays*) under abiotic stresses. *PeerJ* **2023**, *11*, e15312. [\[CrossRef\]](#)
- Song, A.; Wu, D.; Fan, Q.; Tian, C.; Chen, S.; Guan, Z.; Xin, J.; Zhao, K.; Chen, F. Transcriptome-Wide Identification and Expression Profiling Analysis of Chrysanthemum Trihelix Transcription Factors. *Int. J. Mol. Sci.* **2016**, *17*, 198. [\[CrossRef\]](#)
- Zhu, M.; Bin, J.; Ding, H.; Pan, D.; Tian, Q.; Yang, X.; Wang, L.; Yue, Y. Insights into the trihelix transcription factor responses to salt and other stresses in *Osmanthus fragrans*. *BMC Genom.* **2022**, *23*, 334. [\[CrossRef\]](#)
- Li, K.; Fan, Y.; Zhou, G.; Liu, X.; Chen, S.; Chang, X.; Wu, W.; Duan, L.; Yao, M.; Wang, R.; et al. Genome-wide identification, phylogenetic analysis, and expression profiles of trihelix transcription factor family genes in quinoa (*Chenopodium quinoa* Willd.) under abiotic stress conditions. *BMC Genom.* **2022**, *23*, 499. [\[CrossRef\]](#)
- Gao, M.J.; Lydiat, D.J.; Li, X.; Lui, H.; Gjetvaj, B.; Hegedus, D.D.; Rozwadowski, K. Repression of seed maturation genes by a trihelix transcriptional repressor in Arabidopsis seedlings. *Plant Cell* **2009**, *21*, 54–71. [\[CrossRef\]](#)

19. Kitakura, S.; Fujita, T.; Ueno, Y.; Terakura, S.; Wabiko, H.; Machida, Y. The protein encoded by oncogene 6b from *Agrobacterium tumefaciens* interacts with a nuclear protein of tobacco. *Plant Cell* **2002**, *14*, 451–463. [\[CrossRef\]](#)
20. Yu, C.; Song, L.; Song, J.; Ouyang, B.; Guo, L.; Shang, L.; Wang, T.; Li, H.; Zhang, J.; Ye, Z. ShCIGT, a Trihelix family gene, mediates cold and drought tolerance by interacting with SnRK1 in tomato. *Plant Sci.* **2018**, *270*, 140–149. [\[CrossRef\]](#)
21. Yang, L.; Qi, S.; Touqeer, A.; Li, H.; Zhang, X.; Liu, X.; Wu, S. SlGT11 controls floral organ patterning and floral determinacy in tomato. *BMC Plant Biol.* **2020**, *20*, 562. [\[CrossRef\]](#)
22. Fang, Y.; Xie, K.; Hou, X.; Hu, H.; Xiong, L. Systematic analysis of GT factor family of rice reveals a novel subfamily involved in stress responses. *Mol. Genet. Genom.* **2010**, *283*, 157–169. [\[CrossRef\]](#)
23. Li, Y.; Hu, Z.; Dong, Y.; Xie, Z. Trihelix Transcriptional Factor GhGT26 of Cotton Enhances Salinity Tolerance in Arabidopsis. *Plants* **2022**, *11*, 2694. [\[CrossRef\]](#)
24. Liu, X.; Wu, D.; Shan, T.; Xu, S.; Qin, R.; Li, H.; Negm, M.; Wu, D.; Li, J. The trihelix transcription factor OsGTγ-2 is involved adaption to salt stress in rice. *Plant Mol. Biol.* **2020**, *103*, 545–560. [\[CrossRef\]](#)
25. Wang, X.H.; Li, Q.T.; Chen, H.W.; Zhang, W.K.; Ma, B.; Chen, S.Y.; Zhang, J.S. Trihelix transcription factor GT-4 mediates salt tolerance via interaction with TEM2 in Arabidopsis. *BMC Plant Biol.* **2014**, *14*, 339. [\[CrossRef\]](#)
26. Xu, H.; Shi, X.; He, L.; Guo, Y.; Zang, D.; Li, H.; Zhang, W.; Wang, Y. Arabidopsis thaliana Trihelix Transcription Factor AST1 Mediates Salt and Osmotic Stress Tolerance by Binding to a Novel AGAG-Box and Some GT Motifs. *Plant Cell Physiol.* **2018**, *59*, 946–965. [\[CrossRef\]](#)
27. Yoo, C.Y.; Pence, H.E.; Jin, J.B.; Miura, K.; Gosney, M.J.; Hasegawa, P.M.; Mickelbart, M.V. The Arabidopsis GTL1 transcription factor regulates water use efficiency and drought tolerance by modulating stomatal density via transrepression of SDD1. *Plant Cell* **2010**, *22*, 4128–4141. [\[CrossRef\]](#)
28. Luo, J.; Tang, S.; Mei, F.; Peng, X.; Li, J.; Li, X.; Yan, X.; Zeng, X.; Liu, F.; Wu, Y.; et al. BnSIP1-1, a Trihelix Family Gene, Mediates Abiotic Stress Tolerance and ABA Signaling in Brassica napus. *Front Plant Sci.* **2017**, *8*, 44. [\[CrossRef\]](#)
29. Zheng, X.; Liu, H.; Ji, H.; Wang, Y.; Dong, B.; Qiao, Y.; Liu, M.; Li, X. The Wheat GT Factor TaGT2L1D Negatively Regulates Drought Tolerance and Plant Development. *Sci. Rep.* **2016**, *6*, 27042. [\[CrossRef\]](#)
30. Xie, Z.M.; Zou, H.F.; Lei, G.; Wei, W.; Zhou, Q.Y.; Niu, C.F.; Liao, Y.; Tian, A.G.; Ma, B.; Zhang, W.K.; et al. Soybean Trihelix transcription factors GmGT-2A and GmGT-2B improve plant tolerance to abiotic stresses in transgenic Arabidopsis. *PLoS ONE* **2009**, *4*, e6898. [\[CrossRef\]](#)
31. Zhang, Q.; Zhong, T.; E, L.; Xu, M.; Dai, W.; Sun, S.; Ye, J. GT Factor ZmGT-3b Is Associated With Regulation of Photosynthesis and Defense Response to Fusarium graminearum Infection in Maize Seedling. *Front Plant Sci.* **2021**, *12*, 724133. [\[CrossRef\]](#) [\[PubMed\]](#)
32. Yoo, C.Y.; Mano, N.; Finkler, A.; Weng, H.; Day, I.S.; Reddy, A.S.N.; Poovaiah, B.W.; Fromm, H.; Hasegawa, P.M.; Mickelbart, M.V. A Ca(2+)/CaM-regulated transcriptional switch modulates stomatal development in response to water deficit. *Sci. Rep.* **2019**, *9*, 12282. [\[CrossRef\]](#) [\[PubMed\]](#)
33. Kan, Y.; Mu, X.R.; Gao, J.; Lin, H.X.; Lin, Y. The molecular basis of heat stress responses in plants. *Mol. Plant* **2023**, *16*, 1612–1634. [\[CrossRef\]](#) [\[PubMed\]](#)
34. Arab, M.M.; Brown, P.J.; Abdollahi-Arpanahi, R.; Sohrabi, S.S.; Askari, H.; Aliniaefard, S.; Mokhtassi-Bidgoli, A.; Mesgaran, M.B.; Leslie, C.A.; Marrano, A.; et al. Genome-wide association analysis and pathway enrichment provide insights into the genetic basis of photosynthetic responses to drought stress in Persian walnut. *Hortic. Res.* **2022**, *9*, uhac124. [\[CrossRef\]](#) [\[PubMed\]](#)
35. Arab, M.M.; Askari, H.; Aliniaefard, S.; Mokhtassi-Bidgoli, A.; Estaji, A.; Sadat-Hosseini, M.; Sohrabi, S.S.; Mesgaran, M.B.; Leslie, C.A.; Brown, P.J.; et al. Natural variation in photosynthesis and water use efficiency of locally adapted Persian walnut populations under drought stress and recovery. *Plant Physiol. Biochem.* **2023**, *201*, 107859. [\[CrossRef\]](#) [\[PubMed\]](#)
36. Zhang, C.; Lu, L.; Gong, R.; Su, X.; Liu, F.; Zhang, R.; Hu, J. Conservation and Divergence of the Trihelix Genes in Brassica and Expression Profiles of BnaTH Genes in Brassica napus under Abiotic Stresses. *Int. J. Mol. Sci.* **2022**, *23*, 15766. [\[CrossRef\]](#) [\[PubMed\]](#)
37. He, N.Y.; Chen, L.S.; Sun, A.Z.; Zhao, Y.; Yin, S.N.; Guo, F.Q. A nitric oxide burst at the shoot apex triggers a heat-responsive pathway in Arabidopsis. *Nat. Plants* **2022**, *8*, 434–450. [\[CrossRef\]](#)
38. Lotfi, N.; Vahdati, K.; Amiri, R.; Kholdebarin, B. Drought-induced accumulation of sugars and proline in radicle and plumule of tolerant walnut varieties during germination phase. *Acta Hort.* **2010**, *861*, 289–296. [\[CrossRef\]](#)
39. Lotfi, N.; Soleimani, A.; Vahdati, K.; Çakmakçı, R. Comprehensive biochemical insights into the seed germination of walnut under drought stress. *Sci. Hort.* **2019**, *250*, 329–343. [\[CrossRef\]](#)
40. Zhao, J.; Li, P.; Xia, T.; Wan, X. Exploring plant metabolic genomics: Chemical diversity, metabolic complexity in the biosynthesis and transport of specialized metabolites with the tea plant as a model. *Crit. Rev. Biotechnol.* **2020**, *40*, 667–688. [\[CrossRef\]](#)
41. Zhang, X.; Li, L.; Lang, Z.; Li, D.; He, Y.; Zhao, Y.; Tao, H.; Wei, J.; Li, Q.; Hong, G. Genome-wide characterization of NAC transcription factors in *Camellia sinensis* and the involvement of CsNAC28 in drought tolerance. *Front. Plant Sci.* **2022**, *13*, 1065261. [\[CrossRef\]](#) [\[PubMed\]](#)
42. Zhang, X.; Li, L.; He, Y.; Lang, Z.; Zhao, Y.; Tao, H.; Li, Q.; Hong, G. The CsHSFA-CsJAZ6 module-mediated high temperature regulates flavonoid metabolism in *Camellia sinensis*. *Plant Cell Environ.* **2023**, *46*, 2401–2418. [\[CrossRef\]](#) [\[PubMed\]](#)
43. Zhu, J.K. Abiotic Stress Signaling and Responses in Plants. *Cell* **2016**, *167*, 313–324. [\[CrossRef\]](#) [\[PubMed\]](#)

44. Yang, C.; Shi, D.; Wang, D. Comparative effects of salt and alkali stresses on growth, osmotic adjustment and ionic balance of an alkali-resistant halophyte *Suaeda glauca* (Bge.). *Plant Growth Regulation* **2008**, *56*, 179–190. [\[CrossRef\]](#)
45. Breuer, C.; Kawamura, A.; Ichikawa, T.; Tominaga-Wada, R.; Wada, T.; Kondou, Y.; Muto, S.; Matsui, M.; Sugimoto, K. The trihelix transcription factor GTL1 regulates ploidy-dependent cell growth in the Arabidopsis trichome. *Plant Cell* **2009**, *21*, 2307–2322. [\[CrossRef\]](#) [\[PubMed\]](#)
46. Wen, F.; Xu, L.; Xie, Y.; Liao, L.; Li, T.; Jia, M.; Liu, X.; Wu, X. Identification and in Silico Characterization of GT Factors Involved in Phytohormone and Abiotic Stresses Responses in Brachypodium distachyon. *Int. J. Mol. Sci.* **2019**, *20*, 4115. [\[CrossRef\]](#) [\[PubMed\]](#)
47. Yu, C.; Cai, X.; Ye, Z.; Li, H. Genome-wide identification and expression profiling analysis of trihelix gene family in tomato. *Biochem. Biophys. Res. Commun.* **2015**, *468*, 653–659. [\[CrossRef\]](#) [\[PubMed\]](#)
48. Lam, E.; Chua, N.H. GT-1 binding site confers light responsive expression in transgenic tobacco. *Science* **1990**, *248*, 471–474. [\[CrossRef\]](#)
49. O'Grady, K.; Goekjian, V.H.; Naim, C.J.; Nagao, R.T.; Key, J.L. The transcript abundance of GmGT-2, a new member of the GT-2 family of transcription factors from soybean, is down-regulated by light in a phytochrome-dependent manner. *Plant Mol. Biol.* **2001**, *47*, 367–378. [\[CrossRef\]](#)
50. Hu, J.; Liu, T.; Huo, H.; Liu, S.; Liu, M.; Liu, C.; Zhao, M.; Wang, K.; Wang, Y.; Zhang, M. Genome-wide characterization, evolutionary analysis, and expression pattern analysis of the trihelix transcription factor family and gene expression analysis under MeJA treatment in Panax ginseng. *BMC Plant Biol.* **2023**, *23*, 376. [\[CrossRef\]](#)
51. Magwanga, R.O.; Kirungu, J.N.; Lu, P.; Yang, X.; Dong, Q.; Cai, X.; Xu, Y.; Wang, X.; Zhou, Z.; Hou, Y.; et al. Genome wide identification of the trihelix transcription factors and overexpression of Gh_A05G2067 (GT-2), a novel gene contributing to increased drought and salt stresses tolerance in cotton. *Physiol. Plant* **2019**, *167*, 447–464. [\[CrossRef\]](#)
52. Segarra-Medina, C.; Alseekh, S.; Fernie, A.R.; Rambla, J.L.; Perez-Clemente, R.M.; Gomez-Cadenas, A.; Zandalinas, S.I. Absciscic acid promotes plant acclimation to the combination of salinity and high light stress. *Plant Physiol. Biochem.* **2023**, *203*, 108008. [\[CrossRef\]](#) [\[PubMed\]](#)
53. Singh, A.; Roychoudhury, A. Absciscic acid in plants under abiotic stress: Crosstalk with major phytohormones. *Plant Cell Rep.* **2023**, *42*, 961–974. [\[CrossRef\]](#) [\[PubMed\]](#)
54. Hwang, S.M.; Kim, D.W.; Woo, M.S.; Jeong, H.S.; Son, Y.S.; Akhter, S.; Choi, G.J.; Bahk, J.D. Functional characterization of Arabidopsis HsfA6a as a heat-shock transcription factor under high salinity and dehydration conditions. *Plant Cell Environ.* **2014**, *37*, 1202–1222. [\[CrossRef\]](#) [\[PubMed\]](#)
55. Niu, H.; Xia, P.; Hu, Y.; Zhan, C.; Li, Y.; Gong, S.; Li, Y.; Ma, D. Genome-wide identification of ZF-HD gene family in Triticum aestivum: Molecular evolution mechanism and function analysis. *PLoS ONE* **2021**, *16*, e0256579. [\[CrossRef\]](#) [\[PubMed\]](#)
56. Seo, P.J.; Kim, S.G.; Park, C.M. Membrane-bound transcription factors in plants. *Trends Plant Sci.* **2008**, *13*, 550–556. [\[CrossRef\]](#) [\[PubMed\]](#)
57. Kim, S.G.; Lee, A.K.; Yoon, H.K.; Park, C.M. A membrane-bound NAC transcription factor NTL8 regulates gibberellic acid-mediated salt signaling in Arabidopsis seed germination. *Plant J.* **2008**, *55*, 77–88. [\[CrossRef\]](#) [\[PubMed\]](#)
58. Sun, H.; Xie, Y.; Yang, W.; Lv, Q.; Chen, L.; Li, J.; Meng, Y.; Li, L.; Li, X. Membrane-bound transcription factor TaNTL1 positively regulates drought stress tolerance in transgenic Arabidopsis. *Plant Physiol. Biochem.* **2022**, *182*, 182–193. [\[CrossRef\]](#) [\[PubMed\]](#)
59. Yang, L.; Chen, Y.; Xu, L.; Wang, J.; Qi, H.; Guo, J.; Zhang, L.; Shen, J.; Wang, H.; Zhang, F.; et al. The OsFTIP6-OsHB22-OsMYBR57 module regulates drought response in rice. *Mol. Plant* **2022**, *15*, 1227–1242. [\[CrossRef\]](#)
60. Sheikh Beig Goharri, M.A.; Dejang, A.; Tohidfar, M.; Izadi Darbandi, A.; Carrillo, N.J.; Hajirezaei, M.R.; Vahdati, K. Agrobacterium Mediated Transformation of Somatic Embryos of Persian Walnut Using fld Gene for Osmotic Stress Tolerance. *J. Agric. Sci. Technol.* **2016**, *18*, 423–435.
61. Tzafir, I.; Pena-Muralla, R.; Dickerman, A.; Berg, M.; Rogers, R.; Hutchens, S.; Sweeney, T.C.; McElver, J.; Aux, G.; Patton, D.; et al. Identification of genes required for embryo development in Arabidopsis. *Plant Physiol.* **2004**, *135*, 1206–1220. [\[CrossRef\]](#)
62. Xi, J.; Qiu, Y.; Du, L.; Poovaiah, B.W. Plant-specific trihelix transcription factor AtGT2L interacts with calcium/calmodulin and responds to cold and salt stresses. *Plant Sci.* **2012**, *185*–186, 274–280. [\[CrossRef\]](#) [\[PubMed\]](#)
63. Lin, Z.; Griffith, M.E.; Li, X.; Zhu, Z.; Tan, L.; Fu, Y.; Zhang, W.; Wang, X.; Xie, D.; Sun, C. Origin of seed shattering in rice (*Oryza sativa* L.). *Planta* **2007**, *226*, 11–20. [\[CrossRef\]](#) [\[PubMed\]](#)
64. Chang, J.D.; Huang, S.; Yamaji, N.; Zhang, W.; Ma, J.F.; Zhao, F.J. OsNRAMP1 transporter contributes to cadmium and manganese uptake in rice. *Plant Cell Environ.* **2020**, *43*, 2476–2491. [\[CrossRef\]](#) [\[PubMed\]](#)
65. Wang, Z.; He, Z.; Xu, X.; Shi, X.; Ji, X.; Wang, Y. Revealing the salt tolerance mechanism of Tamarix hispida by large-scale identification of genes conferring salt tolerance. *Tree Physiol.* **2021**, *41*, 2153–2170. [\[CrossRef\]](#) [\[PubMed\]](#)
66. Chen, Y.; Sun, Y.; Wan, H.; Chen, L.; Cao, L.; Zhao, B.; Dong, Y.; Hu, C.; Chen, L.; Liu, Z. Integrative analysis of transcriptome and yeast screening system identified heat stress-responding genes in ryegrass. *Environ. Exp. Bot.* **2023**, *210*, 105333. [\[CrossRef\]](#)
67. Jin, J.; Zhang, H.; Kong, L.; Gao, G.; Luo, J. PlantTFDB 3.0: A portal for the functional and evolutionary study of plant transcription factors. *Nucleic Acids Res.* **2014**, *42*, D1182–D1187. [\[CrossRef\]](#) [\[PubMed\]](#)
68. Birney, E.; Clamp, M.; Durbin, R. GeneWise and Genomewise. *Genome Res.* **2004**, *14*, 988–995. [\[CrossRef\]](#)
69. Chen, C.; Chen, H.; Zhang, Y.; Thomas, H.R.; Frank, M.H.; He, Y.; Xia, R. TBtools: An Integrative Toolkit Developed for Interactive Analyses of Big Biological Data. *Mol. Plant* **2020**, *13*, 1194–1202. [\[CrossRef\]](#)

70. Shi, Y.; Zhang, Y.; Sun, Y.; Xie, Z.; Luo, Y.; Long, Q.; Feng, J.; Liu, X.; Wang, B.; He, D.; et al. Natural variations of OsAUX5, a target gene of OsWRKY78, control the neutral essential amino acid content in rice grains. *Mol. Plant* **2023**, *16*, 322–336. [[CrossRef](#)]
71. Zhao, H.; Yao, P.; Zhao, J.; Wu, H.; Wang, S.; Chen, Y.; Hu, M.; Wang, T.; Li, C.; Wu, Q. A Novel R2R3-MYB Transcription Factor FtMYB22 Negatively Regulates Salt and Drought Stress through ABA-Dependent Pathway. *Int. J. Mol. Sci.* **2022**, *23*, 14549. [[CrossRef](#)]

Disclaimer/Publisher’s Note: The statements, opinions and data contained in all publications are solely those of the individual author(s) and contributor(s) and not of MDPI and/or the editor(s). MDPI and/or the editor(s) disclaim responsibility for any injury to people or property resulting from any ideas, methods, instructions or products referred to in the content.